

Test of extended thick-walled through-diaphragm connection to thick-walled CFT column

Ying Qin ^{*1}, Zhihua Chen ^{2a}, Jingjing Bai ² and Zilin Li ³

¹ School of Civil Engineering, Key Lab of Concrete and Prestressed Concrete Structures of Ministry of Education, Southeast University, Nanjing, China

² Key Laboratory of Coast Civil Structure Safety of China Ministry of Education, Tianjin University, China

² School of Civil Engineering, Tianjin Chengjian University, Tianjin, China

(Received September 28, 2013, Revised July 06, 2014, Accepted June 04, 2015)

Abstract. The strength and stiffness of the steel beams to concrete-filled tubular columns connections are significantly reduced if the thick-walled components are used. However, the thick-walled tubes used for columns can largely reduce the demand for space and increase the strength-to-weight ratio. This paper describes the cyclic performance of extended through-diaphragm connections between steel beams and thick-walled concrete-filled tubular columns improved with fillets around the diaphragm corners. Test on one full-scale connection was conducted to assess the seismic behavior of the connection in terms of strength, stiffness, ductility, deformation, energy dissipation, and strain distribution. It is shown that the fillets and extended through-diaphragm can alleviate the stress concentration in the connection and thus improve the seismic performance. The test results demonstrate that the through-diaphragm connections with thick-walled concrete-filled tubular columns can offer sufficient energy dissipation capacity and ductility appropriate for its potential application in seismic design.

Keywords: CFT column; extended through-diaphragm connection; thick-walled; cyclic loading; experimental behavior; seismic performance

1. Introduction

Tubular steel columns offer excellent architectural and structural merits over conventional open columns, particularly in terms of their strength-to-weight ratio, minor axis resistance, torsional stiffness, and aesthetic appearance (Málaga-Chuquitaype and Elghazouli 2010). In addition, their concrete-filled tubular (CFT) counterparts are becoming increasingly attractive due to the benefit of the tube serving as a convenient formwork for placing the concrete and providing confinement for the cured concrete. By confining the concrete in a CFT, an increase in the compressive strength of concrete will realized in addition to preventing the concrete from spalling while subjected to overload. Moreover, the concrete inside the steel tube acts to restrain the local buckling from occurring in the wall of the steel tube. Therefore, structures with CFT columns are increasingly used in engineering applications such as bridges, high-rise buildings, underwater structures and so

*Corresponding author, Assistant Professor, E-mail: qinying@seu.edu.cn

^a Professor, E-mail: zhchen@tju.edu.cn

on (Bergmann *et al.* 1995, Viest *et al.* 1997, Chen *et al.* 2014). Despite the awareness of these advantages, this type of construction is still not being fully exploited due to the practical difficulties involved in forming appropriate cost-effective and construction-efficient connections between CFT columns and steel H-shaped beams. This dearth of information is even more pronounced with regards to the behavior of square CFT column-to-H-beam connections subjected to cyclic loading.

Eurocode 3 (EC3) Part 1-8 (BS EN 1993-1-8 2005) proposes rules for determining the resistance of fully-welded tubular joints. CIDECT Design Guide 3 (Packer *et al.* 2009) and 8 (Zhao *et al.* 2001) offer some computation methods for a variety of rectangular hollow section welded and bolted joints under static loading and fatigue loading, respectively. However, there is a comparative lack of information on their CFT counterparts. Meanwhile, Eurocode 4 (EC4) Part 1-1 (BS EN 1994-1-1 2004) only provides basic design methods for composite joints.

Fully-welded connections with diaphragms offer practical and economical merits, and they have been widely used for CFT structural systems in civil engineering projects in some Asian countries such as China, Japan, and South Korea (Fukumoto 2005). As shown in Fig. 1, each of them employs a plain internal diaphragm, a through diaphragm, or an external diaphragm. Extensive research has been done to study the experimental behavior of moment connections between CFT columns and steel beams under seismic loading conditions. Research by Azuma *et al.* (2000), Miura and Makino (2001), Iwashita (2002), and Iwashita *et al.* (2003) on welded beam-to-column CFT connections with diaphragms have shown that the use of diaphragms locally stiffens the connection, but also develops a complex stress state and leads to fracture of the beam flange at their weld access holes. Cyclic tests on CFT moment connections were conducted by Nishiyama *et al.* (2004), in which shear yielding occurred in the panel zone. Their test results demonstrated that a ductile hysteretic behavior in the specimens can also be achieved with a weak shear panel. Experimental and analytical studies done by Nie *et al.* (2008a, b) concluded that connections with external diaphragm rather than internal diaphragm have adequate strength, good ductility, and high-energy dissipation capacity. The strength and stiffness are less influenced by the axial load ratio and the dimensions of the exterior diaphragms, but more influenced by the width to thickness ratio of the steel tube under shear failure mode. Lee *et al.* (2010) conducted tests to evaluate the structural performance of the external diaphragm connection details and to verify the equations proposed by the authors. Through the study, the composite effect of the internal anchor, the resistance and stress distribution of the connection, the effective location of welding in connection were analyzed. Rong *et al.* (2012), as well as Qin *et al.* (2014e, f), carried out testing on a considerable number of specimens to investigate the seismic behavior of through-diaphragm connections. Based on the experimental results, it concluded that the flexural strength of the connection was largely contributed by the steel tube and the diaphragm.

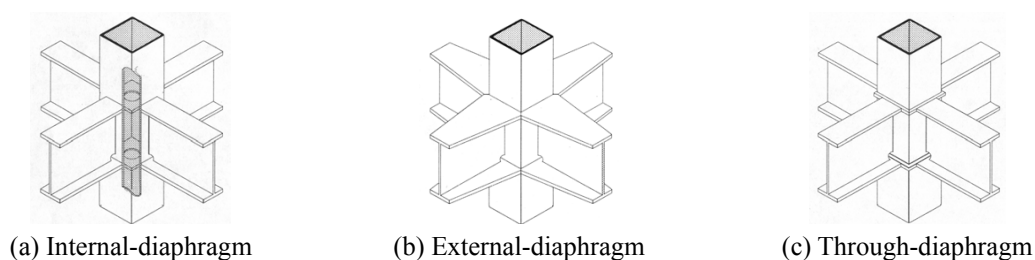


Fig. 1 Traditional details of connections to CFT columns

Previous investigation on the analytical performance of connections with diaphragms has included that of Architectural Institute of Japan (1987), Johansson (2003), Fukumoto and Morita (2005), Nie *et al.* (2009), Wang *et al.* (2009a), Jones and Wang (2010), and Lee and Choi (2012). Architectural Institute of Japan (AIJ) provisions (1987) provide seismic resistance design recommendations. Johansson (2003) conducted a nonlinear finite element study on the mechanical behavior of through-diaphragm connections to CFT columns. The results indicated that the connection should penetrate into the concrete core to distribute load to the concrete when higher demand for load transfer was required. Fukumoto and Morita (2005) proposed a nonlinear shear force-deformation model for the panel zone in beam-to-column CFT connections for predicting the elastoplastic behavior of the panel zones. The proposed model includes a superposed model based on a trilinear shear-deformation relationship for the steel tube superposed on one for the concrete core, and a simple model provided as a trilinear model having a yield strength point and an ultimate strength point for this panel zone, as a practical model for design. Nie *et al.* (2009) established analytical models to calculate the flexural capacity of CFT connections with internal diaphragms or anchored studs, with consideration of the effects of axial load, concrete slab, middle internal diaphragm, beam and column width condition, and punching shear failure mode. Wang *et al.* (2009b, c) performed a series of numerical examples on composite frames with steel beams connected to concrete-filled square hollow section columns. Detailed analysis was carried out on longitudinal stress in steel beam, axial stress distribution in concrete, and concrete stress along the column height and at the connection panel. Parametric studies were conducted to investigate the influence of axial load level, beam-to-column linear stiffness ratio on the structural behavior of composite frames. Numerical models conducted by Jones and Wang (2011) has been developed and used to perform extensive parametric studies. A simple hand calculation method has been developed for evaluating the strength of the column component of rectangular CFTs under tensile load imparted through a fin-plate connection. Lee and Choi (2012) performed finite element analysis to investigate the shear strength under eccentric moment of the CFST column-beam pinned connections. The yield line theory was used to formulate an shear strength formula.

In contrast with these traditional fully welded connections with diaphragms, improvements on them have received relatively less attention. Available studies include the research by Miao and Chen (2011), in which tests were performed on four different through-diaphragm connection configurations including tapered plates, diaphragms of variable cross-section, welded to the face of tubular columns. Good ductility and energy dissipation capability were observed and the influence of connection configurations was highlighted. Shin *et al.* (2004, 2008), as well as Kang *et al.* (2001), evaluated the internal-diaphragm connections reinforced with T-shaped stiffeners with or without holes, based on which three failure modes were identified. Ricles *et al.* (2004) investigated the use of extended tee plates, split-tee plates and tapered plates attached to the beam flange. It was found that panel zone shear yielding and local buckling were ductile modes of response, with minimal strength deterioration occurring in the connection. Cheng *et al.* (2007) performed tests on four steel beams to CFT column connections with floor slabs using taper flange or larger shear tab in the beam-end, in which the development and validation of analytical models for the assessment of the force-deformation behavior of the joint components were conducted.

On the other hand, so far, various connection alternatives to CFT sections have been explored by some researchers such as the use of through-bolt (De Nardin and El Debs 2004, Wu *et al.* 2005), blind bolt (Barnett *et al.* 2001, Loh *et al.* 2006, Wang *et al.* 2009b, c, Tizani *et al.* 2013a, b), combined diaphragm (Choi *et al.* 2006, 2007), bidirectional bolts (Wu *et al.* 2007), asymmetric lower diaphragms (Choi *et al.* 2010), combined channel angle connections (Málaga-Chuquitaype

and Elghazouli 2010), and reinforcing bars and bottom seat-angle (Park *et al.* 2010). Nevertheless, the use of these connection methods has not always been convenient in construction practice and both experimental data and analytical investigation should be expanded. Several state-of-the-art reports and papers also presented a large number of research results on CFT column-to-H-beam connections (Shams and Saadeghvaziri 1997, Shanmugam and Lakshmi 2001, Nishiyama *et al.* 2002, Kurobane 2002, Kurobane *et al.* 2004, Gourley *et al.* 2008).

The most typical details of beam-to-column connections are through-diaphragm connections. The use of through-diaphragm increases the strength and stiffness of the connection most significantly. However, most of the CFT columns in the above research were made of either cold-formed steel (Prabhavathy and Knight 2006, Qin and Chen 2016) or four thin-walled steel plates groove-welded at the corners into a box-shaped cross-section. In contrast, few studies have considered the viability of thick-walled through-diaphragm connections to thick-walled CFT columns, which are beneficial because of their reduction in demand for space and increase in strength-to-weight ratio. Furthermore, connections with thick-walled through-diaphragms and column tubes can be a challenge. The increase in thickness of the steel tube and through-diaphragm leads to an increase in overstress in the steel tube and groove welds of the beam flange due to the lack of flexural capacity of welded connections. This may result in brittle fracture of the connections in an earthquake. In addition, the abrupt change of cross-section from the beam flange to the through-diaphragm in the traditional through-diaphragm connections aggravates the stress concentration there.

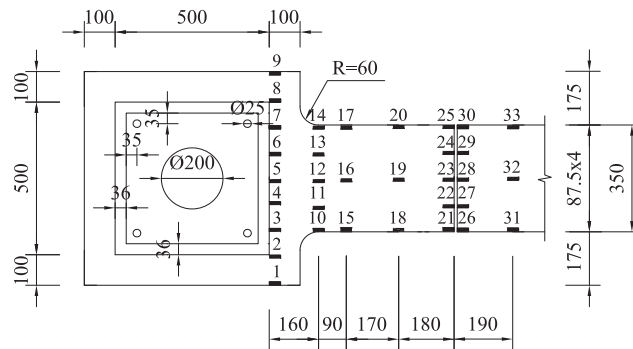
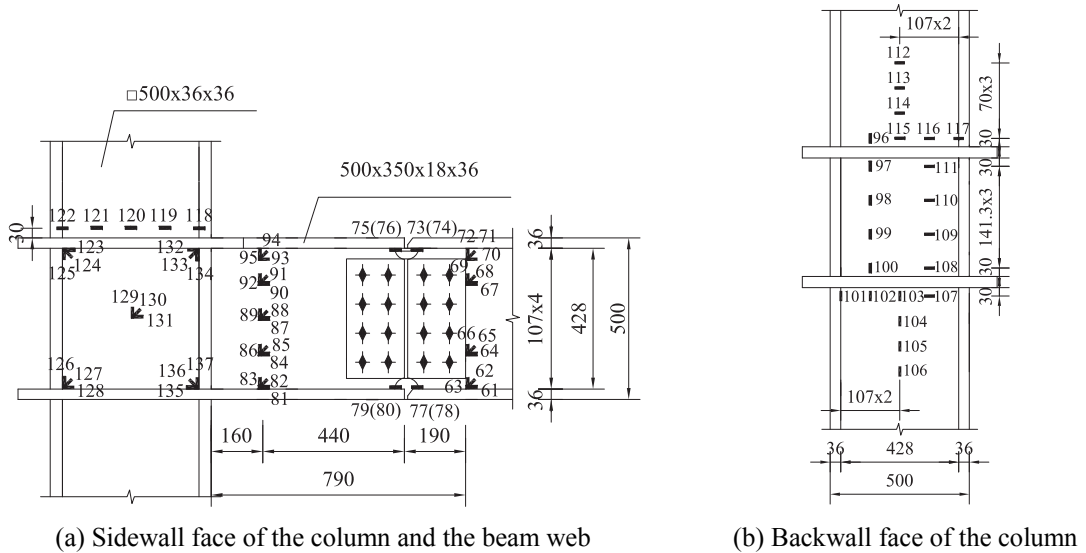
The work presented in this paper attempts to address these issues by investigating the inelastic hysteresis behavior of one proposed through-diaphragm connection to the thick-walled CFT column. The through diaphragms in this study were extended sufficiently far to move the plastic hinge away from the column face. The width of through-diaphragm was gradually decreased towards the end of beam flange. The reduced through-diaphragm cross-section helps alleviate the stress and strain concentration at the beam ends. Additionally, the through-diaphragms had fillets where the cross-section varied to both stiffen the connection and get better performance. The current study involves conducting representative experimental program to examine the seismic behavior of the connection. Based on the experimental results, the cyclic characteristics of the connection are presented and discussed in terms of hysteresis loop, strength, stiffness, deformation, ductility, energy dissipation and strain distribution. The work in this paper provides a basis for further development of a numerical model which will be described in another paper.

2. Experimental program

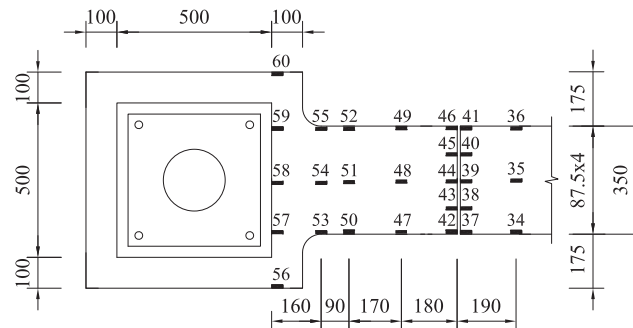
2.1 Test specimen

The program involved the testing of one full-scale connection sample with extended thick-walled through-diaphragm under quasi-static cyclic loading. The case study for this research is Tianjin Library with five stories. The critical governing connection that was subjected to the greatest amount of moment in comparison with both the other connection locations and multiple load combination was selected as the test specimen. The specimen detailing is shown in Fig. 2 and Table 1. The specimen was designed in accordance with the criterion of strong-column- weak-beam, so beam failure mode was expected to occur in the test. The height of the column and the span of the beam were 4200 mm and 3600 mm, respectively. A section of 500 mm (beam depth) ×

350 mm (flange width) × 18 mm (web thickness) × 36 mm (flange thickness) was used for the beam. For the column, a square box section of 500 × 500 × 36 mm was used. The through-diaphragms were 40 mm thick, which was 4 mm thicker than that of beam flange. This thickness



(c) Bottom flange of the beam



(d) Top flange of the beam

Fig. 2 Connection details and layout of strain gauges

Table 1 Summary of test specimen and results

Specimen size (mm)		K_i	M_y	M_u	M_u / M_p	
Specimen section	Length	(kN · m/rad)	(kN · m)	(kN · m)		
Column	□500×500×36	4200	2398	3523	4680	1.72
Beam	500×350×18×36	3600				

was chosen to eliminate through-diaphragm failure and to ensure a strong panel zone. An opening with a diameter of 200 mm was cut out of through-diaphragms for concrete-filling. Four small vent holes with a diameter of 25 mm were also drilled through the walls of the through-diaphragms. These holes were used to release the steam generated in the event of a fire and prevent the column from bursting. The through-diaphragms had fillets at a distance of 100 mm away from the column tube. In order to shift the plastic zone away from the column face, through-diaphragms penetrated the tube column and extended a length of 600 mm. Through-diaphragms and beam flanges were welded to the tube column and through-diaphragms, respectively, using complete joint penetration (CJP) welds. The beam web connection was made with a bolted shear tab. Backing bars were used and left in place throughout the test. Weld tabs were removed after completion of the weld and ground smooth to eliminate notch effects. All the welds were made with the gas shielded flux cored arc welding process using an E50 electrode specified in code for carbon steel covered electrodes GB/T 5117-1995 (1995). Weld access hole detail complied with criteria for rolled shape given in code for welding of steel structures GB 50661-2011 (2011). All CJP welds were made by a certified welder and passed the ultrasonic test.

The high-strength bolts used in the test were Grade 10.9 M22. The mechanical properties of the high-strength bolts were determined from international standard ISO 898-1:2013(E) (2013). The diameter of the bolts was 22 mm, and the ultimate strength and the ratio of the yielding strength to the ultimate strength of the bolts were 1000 N/mm² and 0.9, respectively. The high-strength bolts were initially tightened with a spanner and then with a torque wrench in accordance to the specified torque values listed in the Chinese code for acceptance of construction quality of steel structures GB50205-2001 (2001).

2.2 Material properties

Table 2 summarizes the material properties of the steelwork used throughout the testing program. The mechanical properties for the steel tube, through-diaphragm and H-shaped beam were determined from coupon tensile tests. The geometry of the coupon test piece was specified according to Chinese code GB/T 228-2002 (2002). The compressive strength of the concrete fill was approximately 38.5 N/mm², determined by compressive cube testing.

Table 2 Material properties of steel

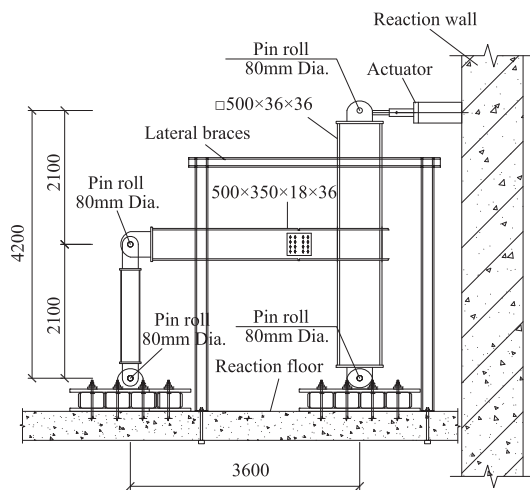
Type	t (mm)	f_y (N/mm ²)	f_u (N/mm ²)	f_y / f_u	$Elo.$ (%)	E_s (×10 ⁵ N/mm ²)
Tube of CFT	36	400.6	541.7	0.74	29.4	1.97
Diaphragm	40	372.9	540.8	0.69	23.1	2.22
Steel beam	-	407.8	554.3	0.74	24.3	2.24

2.3 Test setup and loading

Fig. 3 provides a schematic view of the connection test setup. Due to the limitations of the cost and laboratory testing area, it was not feasible to construct a cruciform shape specimen to analyze the interior connection of the frame. The lateral cyclic load was applied at the top of the CFT column by a 1000 kN actuator. The ends of the specimen were attached to cylindrical bearings and were free to rotate in-plane, and thus simulate pin boundary conditions. Lateral restraint was provided near the beam.

It was worth noting that the axial loading was not applied to the top of the CFT column. The nominal strength of the column N_u was 33,819 kN according to technical specification for structures with concrete-filled rectangular steel tube members CECS 159:2004 (2004). It was not feasible to apply the axial force by a laboratory hydraulic jack to generally reflect the real axial level of the CFT column in a practical building structural system, as the level of axial load (n), $n = N_0 / N_u$, normally ranges from 0.4~0.8, where N_0 = axial compressive strength of the column. The presence of the axial force on the CFT column will affect the seismic performance of the connection, especially for the cumulative damage in the panel zone, which is also stated by Qin *et al.* (2014c, d). Laboratory constraints prohibited the application of axial load to the column. Nevertheless, the effects of column axial loads will be considered and studied in the finite element analysis in a parallel paper.

The lateral loading history of the connection was generally based on the ANSI/AISC 341-10 (2010) guidelines for cyclic testing of structural steel components. The load was controlled by the story drift angle, which was transformed into the displacement at the column tip by multiplying the story drift angle by the column height. Six cycles were imposed at each of the rotation levels of 0.375%, 0.5% and 075%. Four cycles were imposed at the rotation of 1%. After the rotation of 1.5%, it was loaded for 2 cycles at intervals of 1% of the story drift angle until failure of the specimen occurred.



(a) Test setup



(b) Photograph of loading system

Fig. 3 Loading system

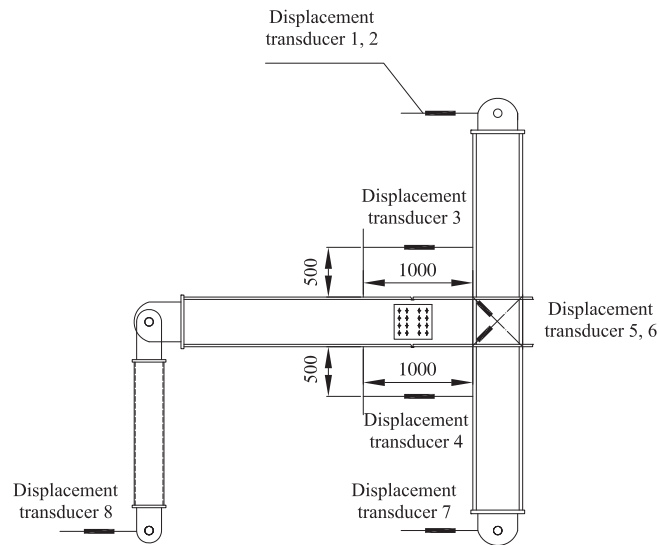


Fig. 4 Layout of displacement transducers

2.4 Instrumentation

A representative layout of the instrumentation adopted in the experimental tests is shown in Fig. 4. The in-plane displacements of the column and steel beam were measured by eight displacement transducers along the connection specimen. Displacement transducers 1 and 2 were used to measure the displacement at the top of the column at the load application point of the MTS hydraulic ram. Displacement transducers 7 and 8 were used to obtain the horizontal movement of the box foundation. Other four displacement transducers were used to calculate the rotation of the connection and the shear deformation in the panel zone.

Strain measurements were also used to measure the strains in the through-diaphragm, the flange and web of the beam, and the backwall and sidewall faces of the CFT column as shown in Fig. 2. The strain measurements on the backwall face of the CFT column were collected in two directions parallel and perpendicular to the through-diaphragm, while those on the sidewall faces of the column and beam web were arranged in three directions using three-elements strain gauges rosette. Single-element strain gauges were placed on the through-diaphragm and beam flanges to monitor the highest strains there and determine the stress transfer under the cyclic loading.

3. Experimental results and discussion

3.1 General observations

The test specimen exhibited ductile behavior and the test proceeded in a smooth and controlled fashion. It was observed that the specimen essentially behaved in an elastic manner at an early stage before the actuator displacement reached a level of 63 mm corresponding to a rotation of 1.5%. In the following successive cycles, the beam flange near the through-diaphragm showed slight local buckling. The test was terminated at a rotation of 4% when an unexpected fracture



Fig. 5 Failure of the test setup

occurred at the bolts which were used to bolt the box foundation to the reaction floor, as shown in Fig. 5. That is to say, the failure was caused not by the failure of the specimen, but by the failure of the test setup. However, the test was not continued because it was believed that the sudden dynamics impact has led to the interior defect in the connection. The hysteresis characteristics of the proposed connection will be discussed up to this “failure” point in the following sections, although the connection could potentially exhibit significantly better seismic performance.

3.2 Moment-rotation response

The performance of the beam-to-column connection is critically important to the response of composite frame, and is largely dependent on the moment-rotation response. The connection rotation and the corresponding moment was used to construct the hysteresis moment-rotation curve of the test specimen shown in Fig. 6, where the moment is calculated by the lateral load multiplied by the height of the column, and the rotation is obtained by the horizontal displacement measured at the top of the column divided by the height of the column. To obtain the moment strength and the initial stiffness of the specimen, the moment-rotation hysteresis curve was converted to the equivalent moment-rotation envelop curve (see Fig. 6). The yield moment (M_y), ultimate moment (M_u) and initial stiffness (K_i) are summarized in Table 1.

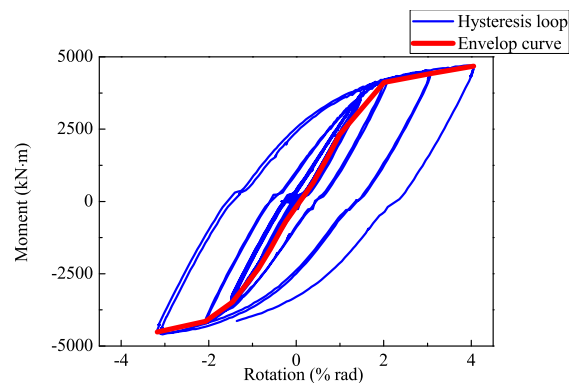


Fig. 6 Moment-rotation relationship

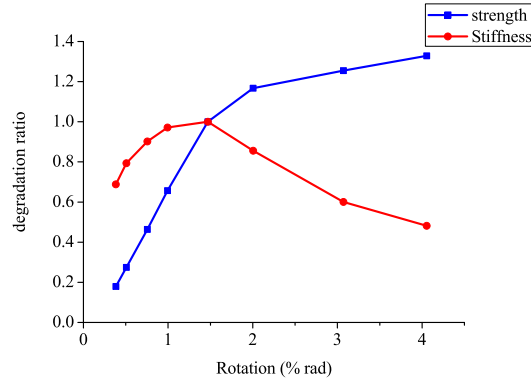


Fig. 7 Strength and stiffness degradation

It can be seen that the behavior of the connection was initially elastic, followed by an inelastic response with gradually decreasing stiffness, until the failure occurred. The hysteresis curve for the test exhibited stable behavior without noticeable pinching effect. It should also be noted that no decline curve was observed due to the fact that no axial force was applied to the CFT column.

The ultimate moment capacity of the specimen was 4680 kN·m, which was well over the calculated full plastic moment (M_p) of the bare beam. Consequently, the connection exhibited good hysteresis behavior of resistance under cyclic bending.

3.3 Strength and stiffness degradation

Strength degradation is a key element to evaluate the performance of connections under cyclic loadings such as earthquake ground motions. It is evaluated by using the strength degradation ratio (λ_i), which is the ratio of the moment amplitude at the rotation of i to the initial yield moment (Tizani *et al.* 2013a).

The strength degradation in Fig. 7 indicates that no obvious degradation of strength was noticed before failure. It showed a gradual and stable growth in strength as the test progressed. This can be explained by the absence of axial load on the column (Han *et al.* 2011), which leads to the curve stably going up strengthening stage.

Connections with large degree of stiffness degradation tend to exhibit larger rotations under cyclic loads that may lead to extensive damage to other structural elements (Tizani *et al.* 2013a). Stiffness degradation (ξ) is defined as the ratio of the secant stiffness at rotation of i to the initial stiffness (Tang 1989).

During the test the stiffness of the specimen decreased due to the cumulative damage as the cyclic loading progressed. It is shown in Fig. 7 that the stiffness of the specimen had an almost linear descending tendency from the yielding point up to the failure point, which indicates a modest deterioration of the hysteresis loop in the connection. However, Fig. 7 shows a stable increase in the stiffness during the first several cycles. The unexpected growth can be attributed to the fact that the specimen and the test setup had not been structurally tight. This leads to a relatively large rotation corresponding to certain load level and consequently results in a small value of stiffness. Additionally, the results demonstrate a larger rate of degradation of stiffness compared with strength. This can be easily explained as the cumulative plastic deformation has significant effect on the stiffness of the connection, and also the contribution of the concrete infill

to the stiffness is reduced as a result of potential damage to the concrete. In general, it can be concluded that the stiffness degradation is more significant than the strength degradation.

3.4 Deformation analysis and $Q_H - \gamma_j$ curves

When the specimen is loaded under horizontal cyclic loading, every component of the connection deforms (Nie *et al.* 2008a). So the local plastic mechanisms in the structure can be localized not only at the beam or column end, but also at joints, or at both, member ends and joints (Mazzolani 2000). As for an exterior connection, the displacement at the top of the column Δ can be separated into three components attributed to the deformation due to the column (Δ_c), the beam (Δ_b), and the panel zone (Δ_j), as shown in Fig. 8. Fig. 9 illustrates the deformation analysis results, where $r_{\Delta_j} = \Delta_j/\Delta$, $r_{\Delta_c} = \Delta_c/\Delta$, $r_{\Delta_b} = \Delta_b/\Delta$.

Since the specimen was designed according to the requirement of strong panel zone, the displacement ratio caused by the panel zone was the smallest and remained approximately constant. At the end of the test, r_{Δ_j} is 2.5%, while the percentages of total displacement contributed by the beam and the column were 36.7%, 60.8%, respectively. The results indicate that the shear deformation in the panel zone developed insufficiently. The displacement ratio caused by the beam steadily grew larger with the increase in loading until the displacement reached 89 mm. The corresponding maximum r_{Δ_b} was almost 73%. Then the value of v stably decreased. This may be attributed to the potential crush of concrete infill of the column and the ensuing loss of stiffness.

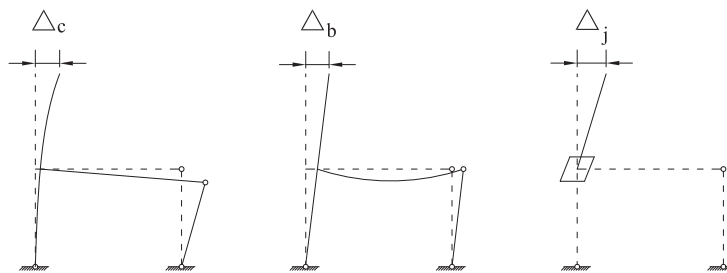


Fig. 8 Deformation analysis

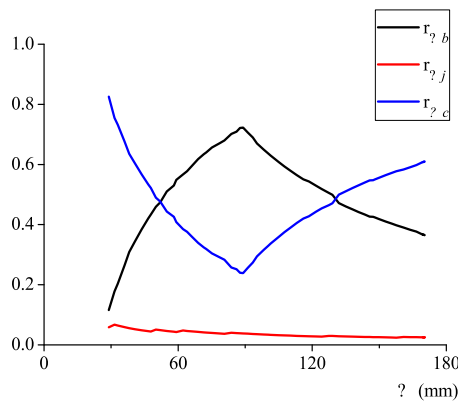
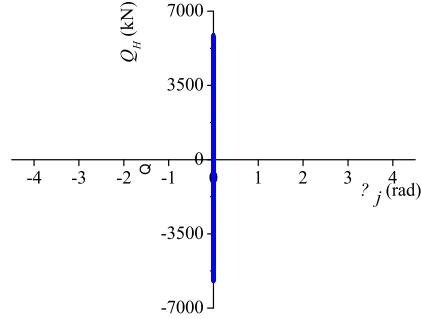


Fig. 9 $r_{\Delta} - \Delta$ curve

Fig. 10 $Q_H - \gamma_j$ hysteresis loop

In order to investigate the performance of the panel zone of the connection, $Q_H - \gamma_j$ hysteresis loop of the specimen is shown in Fig. 10.

Q_H is the shear force in the panel zone. As stated by Li and Li (2007), the three edges of a beam-to-column exterior joint panel zone are subjected to the reaction forces from beams and columns connected to the joint panel, as shown in Fig. 11, where M_b and Q_b are, respectively, the moment and shear from the beam end, and M_{cT} , Q_{cT} , N_{cT} , M_{cB} , Q_{cB} and N_{cB} are, respectively, the moments, shears and thrusts from the top and bottom column ends. All these actions make the joint panel in a shear state. The equivalent horizontal shear force in the panel zone can be written as Eq. (1)

$$Q_H = -\frac{M_b}{h_g} + \frac{1}{2}(Q_{cB} - Q_{cT}) \quad (1)$$

γ_j is the shear deformation of the panel zone as shown in Fig. 12. It can be derived from Eq. (2)

$$\gamma_j = \frac{1}{2}(\Delta_1 + \Delta_2 + \Delta_3 + \Delta_4) \frac{\sqrt{a^2 + b^2}}{ab} \quad (2)$$

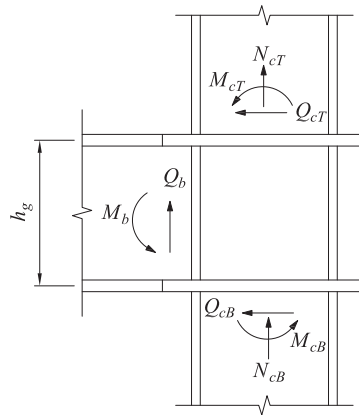


Fig. 11 Forces applied on a joint panel

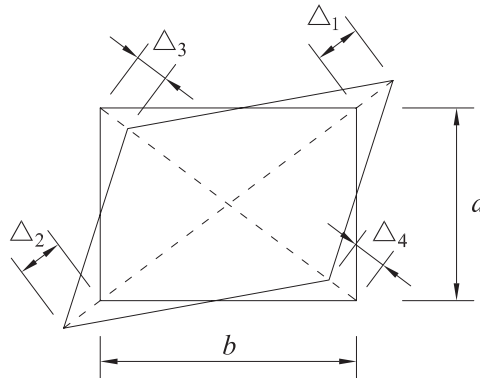


Fig. 12 Shear distortion in the panel zone

Table 3 Ductility ratios and drift rotation

$\mu (+)$	$\mu (-)$	θ (rad)	$\theta_e / [\theta_e]$	$\theta_p / [\theta_p]$
3.10	2.46	0.03	3.93	2.03

* Note: θ_e = elastic story drift rotation; θ_p = elasto-plastic story drift rotation

The hysteresis loop of the connection was almost linear, and the maximum shear deformation in the panel zone was less than 6×10^{-4} rad. Therefore, it can be concluded that the panel zone of this type of connection remained in the elastic range all the time. This shows the development of a rigid panel zone as expected. The experimental shear stiffness was achieved from regression analysis within the elastic stage. This value was significantly less than the theoretical one that was derived from the equations proposed by Fukumoto and Morita (2005), as the ultimate shear strength of the panel zone was not reached in the test based on the design criterion of strong panel zone. This can also be verified by the fact that during the test no yielding of panel zone had been observed.

3.5 Ductility and story drift angle

Ductility is defined as the ability of the connections to undergo large plastic deformation without obvious loss of strength (Mazzolani 2000). It is an important parameter in earthquake-resistant design of structures. According to Tizani *et al.* (2013a), the assessment of ductility for connections can be carried out by calculating ductility ratio, which is defined as the ratio of the ultimate rotation to the yielding one. The ductility ratio shows the capability of the connection to accept nonlinear rotations without extensive damage. Table 3 lists the ultimate rotation (θ) and ductility ratio (μ), where (+) denotes the upper semi-cycles and (-) denotes the lower semi-cycles. As expected, the specimen exhibited good ductility. The ductility ratio of the connection was over 2.

In an earthquake, the ability of inelastic deformation to absorb large amounts of energy and shear force is critical to the stability of the column-to-beam connection of the structure. Table 4 presents the total drift angle required for the moment frame according to the AISC seismic provisions for structural steel buildings (ANSI/AISC 341-10 2010). The total rotation of the

Table 4 Rotation capacity requirements for composite connections

Frame classifications	Connection rotation capacity (rad)
Composite ordinary moment frame (C-OMF)	0.02
Composite intermediate moment frame (C-IMF)	0.03
Composite special moment frame (C-SMF)	0.04

connection is based on the last successful cycle that was achieved before failure and the data is listed in Table 3. In a typical moment frame where points of deflection of the beams and columns are located at their mid-points under cyclic lateral loading, a total rotation of 3% rad is comparable to a story drift angle of 3% rad. Note that no obvious crack or failure were observed at the end of the test, which means the specimen could potentially reach a much larger rotation angle. Therefore, the specimen meets the requirement for the composite intermediate moment frame in any case.

Based on the Chinese code for the seismic design of buildings GB50011-2001 (2008), the limit value of elastic story drift rotation $[\theta_e]$ and the limit value of elasto-plastic story drift rotation $[\theta_p]$ are determined as follows: for multi-story and tall steel structures, $[\theta_e] = 1/300$ and $[\theta_p] = 1/50$, respectively. As can be seen in Table 3, the specimen satisfies the requirement for seismic deformation checks.

3.6 Energy dissipation capacity

The inelastic deformation of the connections aids the energy dissipation through hysteresis behavior, thereby reducing the transmitted energy to other structural components. This can help to improve the seismic performance of the whole structural system subjected to strong earthquakes (Tizani *et al.* 2013a). According to Tizani *et al.* (2013a), the energy absorbed by the deformation of the connection can be measured as the areas enclosed by the moment-rotation hysteresis curve. This is the total plastic work performed by the specimen. The equivalent damping coefficients of the test specimen at the rotation of 1.5%, 2%, 3% are 0.04, 0.11, 0.21, respectively.

As expected, the energy dissipation of the connection gradually increased by increasing the load amplitudes up to the failure point. Comparing the final value of the equivalent damping coefficient with the results of the concrete connections and concrete encased steel column connections (Zhou *et al.* 2004), it demonstrates that the energy dissipation capacity of the extended thick-walled through-diaphragm connection to thick-walled CFT column is much higher than that of the concrete connections, and it is close to that of the concrete encased steel column connections, which is consistent with the observation by Qin *et al.* (2014a, b) and indicates to some extent that, the deformation abilities of the two typical steel-concrete composite systems, i.e., the concrete-filled tube systems and the concrete encased steel systems, are almost the same.

The results of this study indicate that the new extended thick-walled through-diaphragm connection to thick-walled CFT column, in general, can offer sufficient energy dissipation capacity which makes it suitable for seismic applications.

3.7 Strain distribution

The strain distribution of the specimen is analyzed until a rotation angle of 1.5% rad was reached. The value of 1.5% rad was selected because the yielding of the specimen occurred at this level of rotation, although the specimen could potentially reach a rotation of 3% or more. For ease

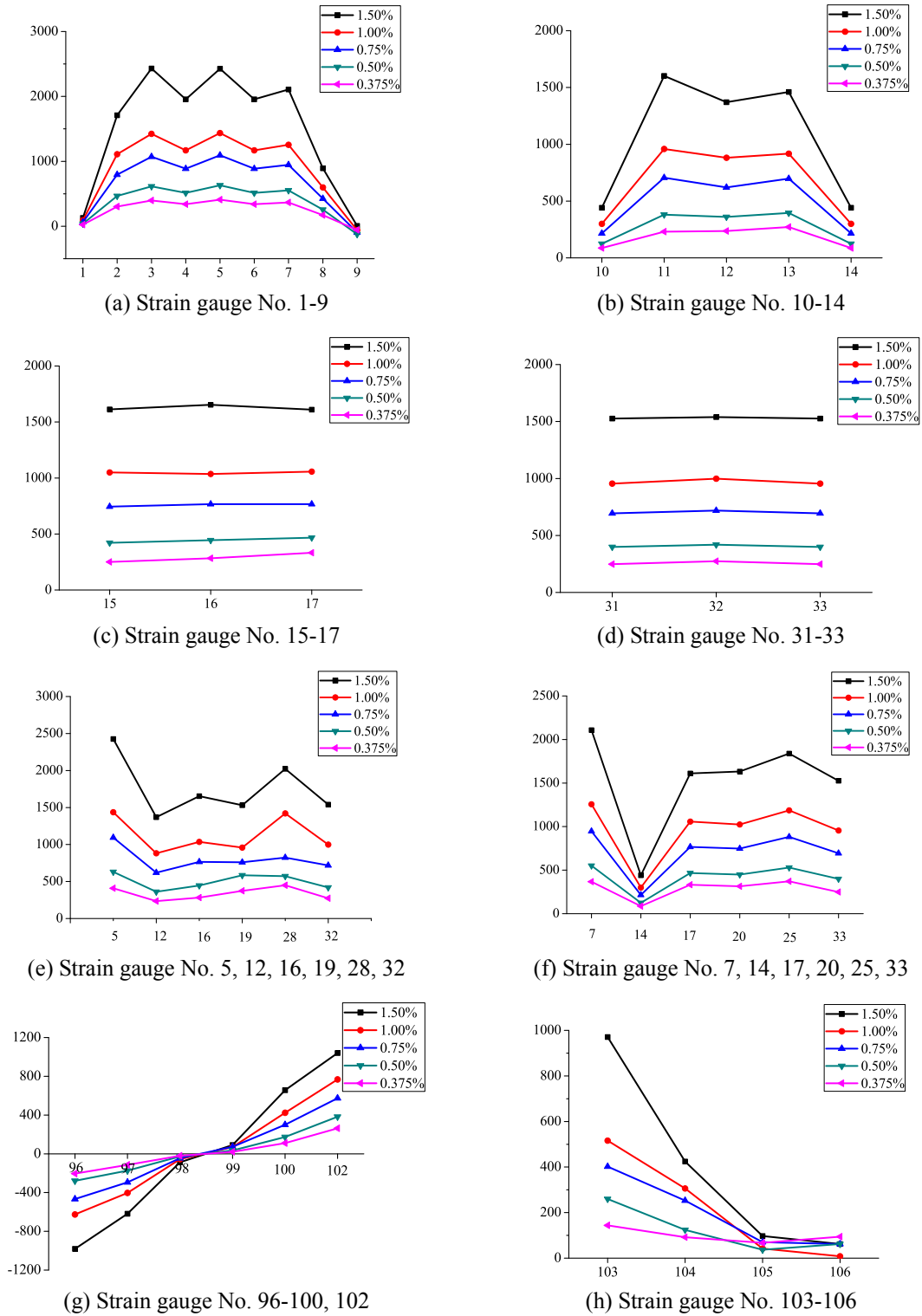


Fig. 13 Strain distribution

of presentation, only the strains of critical points are discussed below. The measured strains in the specimen are shown in Fig. 13, where the positive values denote the tensile strains, and negative values denote the compressive strains. The behavior was plotted at the points of each rotation amplitude.

Figs. 13(a)-(d) illustrate the typical strain distribution measured along the transverse direction of the through-diaphragm and steel beam at different position along its span. It demonstrates that the strains were uniformly distributed along the width far away from the column (see Figs. 13(c) and (d)). Nevertheless, an evidently non-uniform strain distribution was observed in the through-diaphragm adjacent to the column face, due to the largest moment there and more extensive inelastic yielding of the through-diaphragm. It was also worth noting that the values of strains at both sides of through-diaphragm were almost zero, while the strain in the center was the highest. Strain gauge readings reveal that a shear lag phenomenon developed along the width of through-diaphragm. It is evident that a negligible amount of force was transferred from the sides of the through-diaphragm to the sides of the steel tube that formed the connection's panel zone.

The variation of the strains in the center of through-diaphragm and beam flange along the longitudinal direction against the rotation is shown in Fig. 13(e). There was a significant increase in the strains of the CPJ welds that connected the beam flange to the through-diaphragm as a result of the strain concentration at the welds. Fig. 13(f) shows a very consistent and similar behaviour except for a sharp decrease in the strain where the cross-section of the through-diaphragm changed. It indicates that the improvement to connection configuration (fillets and extended through-diaphragm in this paper) can largely affect the strain distribution and significantly alleviate the stress concentration. Furthermore, this result implies that these connection details significantly helps build a more uniform stress distribution.

Figs. 13(g)-(h) show the response of the strains of the backwall side of the column. It should be noted that the strain levels of the column were obviously less than those for the beam and through-diaphragm. It can be seen from Fig. 13(g) that the strains were linearly distributed over the flange of the column along the column height close to the panel zone all the time. However, the strains in the column flange steadily decreased to almost zero at a distance of 240 mm, or 6 times the thickness of column tube, away from the bottom flange of the beam as show in Fig. 13(h), this phenomenon illustrates that the tensile and compressive force transferred from the beam flange only affect the behaviour of the CFT column within a certain length.

In general, the test results indicate that the specimen with thick-walled CFT column and extended thick-walled diaphragm is able to perform as good as, if not better than the traditional through-diaphragm connections with identical beam and column length (Qin *et al.* 2014a). The moment-rotation hysteresis behavior, strength and stiffness degradation and the energy dissipation capacity of the thick-walled connection are similar to those of traditional type connections, while the ductility ratio and the total story drift angle of the thick-walled specimen are even higher. It worth noting that increased testing repetitions may be necessary to establish more reliable results. Furthermore, the welding residual stress can have great impact on the seismic performance of the connection, which cannot be quantified based on the test data only. The experimental results and related analysis in this paper however, can be taken as a basic reference for the application of this innovative extended thick-walled through-diaphragm connection to thick-walled CFT column. Development of detailed finite element and analytical models to simulate the hysteresis performance of this type of connection will be discussed in a companion paper.

4. Conclusions

To investigate the cyclic performance of the extended thick-walled through-diaphragm connections to thick-walled CFT columns, one full-scale subassembly test was conducted under cyclic loading. Based on the test results, the following conclusions are made:

- (1) Fillets of the through-diaphragm at the corners reduced stress concentrations at those locations and improved the cyclic performance.
- (2) The extended through-diaphragm contributed to the more uniformly distributed strains and significantly decreased the stress concentration in the through-diaphragm adjacent to the column.
- (3) The specimen achieved the required 0.03 rad of total rotation for composite intermediate moment frame. It appears that better performance might be possible as the test was terminated by the failure of the test setup. Therefore, the specimen has the potential to reach a much higher rotation and to be applied for composite special moment frame, which needs further investigation in the future.
- (4) The total displacement of the connection was largely contributed by the deformation of the column and beam. This demonstrates that more yielding occurred there. Furthermore, the degradation of stiffness was more significant than the degradation of strength in the proposed specimen.
- (5) The connection strength of the specimen was well above the full plastic moment strength of the bare beam, and the moment-rotation curve showed plentiful hysteresis behavior without pinching. The proposed connection exhibited sufficient ductility and energy dissipation capacity under cyclic loading.

Acknowledgments

This work is sponsored by the National Natural Science Foundation of China (Grant No. NSFC61272264) and A Project Funded by the Priority Academic Program Development of Jiangsu Higher Education Institutions (PAPD). The authors also appreciate the financial support provided by the Chinese Scholarship Council (File No. 201206250067) that enables the Visiting Research Scholar to cooperate with Dr. Benjamin W. Schafer at Johns Hopkins University at Baltimore.

References

- ANSI/AISC 341-10 (2010), Seismic Provisions for Structural Steel Buildings, American Institute of Steel Construction, Inc., Chicago, IL, USA.
- Architectural Institute of Japan (1987), AIJ Standard for Structural Calculation of Steel Reinforced Concrete Structures, Architectural Institute of Japan, Tokyo, Japan.
- Azuma, K., Kurobane, Y. and Makino, Y. (2000), "Cyclic testing of beam-to-column connections with weld defects and assessment of safety of numerically modeled connections from brittle fracture", *Eng. Struct.*, **22**(12), 1596-1608.
- Barnett, T.C., Tizani, W. and Nethercot, D.A. (2001), "The practice of blind bolting connections to structural hollow sections: A review", *Steel Compos. Struct., Int. J.*, **1**(1), 1-16.
- Bergmann, R., Matsui, C., Meinsma, C. and Dutta, D. (1995), Design Guide for Concrete Filled Section Columns under Static and Seismic Loading, CIDECT Design Guide No. 5, CIDECT and Verlag TÜV Rheinland GmbH, Köln, Germany.

- BS EN 1993-1-8 (2005), Eurocode 3: Design Provision of Steel Structures-Part 1-8: Design of Joints, British Standards Institution, UK.
- BS EN 1994-1-1 (2004), Eurocode 4: Design of Composite Steel and Concrete Structures, Part 1-1: General Rules and Rules for Buildings, British Standards Institution, UK.
- CECS 159:2004 (2004), Technical Specification for Structures with Concrete-Filled Rectangular Steel Tube Members, China Planning Press, Beijing, China.
- Chen, Z., Qin, Y. and Wang, X. (2014), "Development of connections to concrete-filled rectangular tubular columns", *Adv. Steel Constr.*, **11**(4), 408-426.
- Cheng, C.T., Chan, C.F. and Chung, L.L. (2007), "Seismic behavior of steel beams and CFT column moment-resisting connections with floor slabs", *J. Constr. Steel Res.*, **63**(11), 1479-1493.
- Choi, S., Yun, Y. and Kim, J. (2006), "Experimental study on seismic performance of concrete filled tubular square column-to-beam connections with combined cross diaphragm", *Steel Compos. Struct., Int. J.*, **6**(4), 303-317.
- Choi, S., Jung, D., Kim, D. and Kim, J. (2007), "An evaluation equation of load capacities for CFT square column-to-beam connections with combined diaphragm", *Steel Compos. Struct., Int. J.*, **7**(4), 303-320.
- Choi, S.M., Park, S.H. and Yun, Y.S. (2010), "A study on the seismic performance of concrete-filled square steel tube column-to-beam connections reinforced with asymmetric lower diaphragms", *J. Constr. Steel Res.*, **66**(7), 962-970.
- De Nardin, S. and El Debs, A.L.H.C. (2004), "An experimental study of connections between I-beams and concrete filled steel tubular columns", *Steel Compos. Struct., Int. J.*, **4**(4), 303-315.
- Fukumoto, T. (2005), "Steel-beam-to-concrete-filled-steel-tube-column moment connections in Japan", *Steel Struct.*, **5**(4), 357-365.
- Fukumoto, T. and Morita, K. (2005), "Elastoplastic behavior of panel zone in steel beam-to-concrete filled steel tube column moment connections", *J. Struct. Eng.*, **131**(12), 1841-1853.
- GB/T 5117-1995 (1995), Carbon Steel Covered Electrodes, Standards Press of China, Beijing, China.
- GB 50205-2001 (2002), Code for Acceptance of Construction Quality of Steel Structures, China Planning Press, Beijing, China.
- GB/T 228-2002 (2002), Metallic Materials-Tensile Testing at Ambient Temperature, Standards Press of China, Beijing, China.
- GB50011-2001 (2008), Code for Seismic Design of Buildings, China Architecture and Building Press, Beijing, China.
- GB 50661-2011 (2011), Code for Welding of Steel Structures, China Architecture and Building Press, Beijing, China.
- Gourley, B.C., Tort, C., Denavit, M.D., Schille, P.H. and Hajjar, J.F. (2008), "A synopsis of studies of the monotonic and cyclic behavior of concrete-filled steel tube members, connections, and frames", NSEL report series, Report no. NSEL-008; Department of Civil and Environmental Engineering, University of Illinois at Urbana-Champaign, IL, USA.
- Han, L.H., Wang, W.D. and Tao, Z. (2011), "Performance of circular CFST column to steel beam frames under lateral cyclic loading", *J. Constr. Steel Res.*, **67**(5), 876-890.
- ISO 898-1:2013(E) (2013), Mechanical Properties of Fasteners Made of Carbon Steel and Alloy Steel Part 1: Bolts, Screws and Studs with Specified Property Classes-Coarse Thread and Fine Pitch Thread, British Standards Institution, Switzerland.
- Iwashita, T. (2002), "Brittle fracture from ends of CJP groove welded joints", *Proceedings of the 12th International Offshore and Polar Engineering Conference*, Kitakyushu, Japan, May.
- Iwashita, T., Kurobane, Y., Azuma, K. and Makino, Y. (2003), "Prediction of brittle fracture initiating at ends of CJP groove welded joints with defects: Study into applicability of failure assessment diagram approach", *Eng. Struct.*, **25**(14), 1815-1826.
- Johansson, M. (2003), "Composite action in connection regions of concrete-filled steel tube columns", *Steel Compos. Struct., Int. J.*, **3**(1), 47-64.
- Jones, M.H. and Wang, Y.C. (2010), "Tying behaviour of fin-plate connection to concrete-filled rectangular steel tubular column - Development of a simplified calculation method", *J. Constr. Steel Res.*, **66**(1), 1-10.

- Kang, C.H., Shin, K.J., Oh, Y.S. and Moon, T.S. (2001), "Hysteresis behavior of CFT column to H-beam connections with external T-stiffeners and penetrated elements", *Eng. Struct.*, **23**(9), 1194-1201.
- Kurobane, Y. (2002), "Connections in tubular structures", *Prog. Struct. Eng. Mater.*, **4**(1), 35-45.
- Kurobane, Y., Packer, J.A., Wardenier, J. and Yeomans, N. (2004), Design Guide for Structural Hollow Section Column Connections, CIDECT Design Guide No. 9, CIDECT and Verlag TÜV Rheinland GmbH, Köln, Germany.
- Lee, Y.K. and Choi, S. (2012), "Shear strength formula of CFST column-beam pinned connections", *Steel Compos. Struct., Int. J.*, **11**(5), 409-421.
- Lee, S., Yang, S. and Choi, S. (2010), "Structural characteristics of welded built-up square CFT column-to-beam connections with external diaphragms", *Steel Compos. Struct., Int. J.*, **10**(3), 261-279.
- Li, G.Q. and Li, J.J. (2007), *Advanced Analysis and Design of Steel Frames*, John Wiley & Sons, Ltd., Hoboken, NJ, USA.
- Loh, H.Y., Uy, B. and Bradford, M.A. (2006), "The effects of partial shear connection in composite flush end plate joints Part I - experimental study", *J. Constr. Steel Res.*, **62**(4), 378-390.
- Málaga-Chuquitaype, C. and Elghazouli, A.Y. (2010), "Behaviour of combined channel/angle connections to tubular columns under monotonic and cyclic loading", *Eng. Struct.*, **32**(6), 1600-1616.
- Mazzolani, F.M. (2000), *Moment Resistant Connections of Steel Frames in Seismic Areas: Design and Reliability*, E&FN Spon Press, New York, NY, USA.
- Miao, J.K. and Chen, Z.H. (2011), "Seismic behavior of concrete-filled square steel tubular column-to-beam connections with through diaphragm", *Adv. Struct. Eng.*, **94-96**, 1344-1351.
- Miura, K. and Makino, Y. (2001), "Testing of beam-to-RHS column connections without weld access holes", *Proceedings of the 11th International Offshore and Polar Engineering Conference*, Stavanger, Norway, June.
- Nie, J.G., Qin, K. and Cai, C.S. (2008a), "Seismic behavior of connections composed of CFSSTCs and steel-concrete composite beams - experimental study", *J. Constr. Steel Res.*, **64**(10), 1178-1191.
- Nie, J.G., Qin, K. and Cai, C.S. (2008b), "Seismic behavior of connections composed of CFSSTCs and steel-concrete composite beams - finite element analysis", *J. Constr. Steel Res.*, **64**(6), 680-688.
- Nie, J.G., Qin, K. and Cai, C.S. (2009), "Seismic behavior of composite connections - flexural capacity analysis", *J. Constr. Steel Res.*, **65**(5), 1112-1120.
- Nishiyama, I., Morino, S., Sakino, K., Nakahara, H., Fujimoto, T., Mukai, A., Inai, E., Makoto, K., Tokinoya, H., Fukumoto, T., Mori, K., Yoshioka, K., Mori, O., Yonezawa, K., Uchikoshi, M. and Hayashi, Y. (2002), "Summary of research on concrete-filled structural steel tube column system carried out under the US-Japan cooperative research program on composite and hybrid structures", BRI research paper no.147, Building Research Institute, Japan.
- Nishiyama, I., Fujimoto, T., Fukumoto, T. and Yoshioka, K. (2004), "Inelastic force-deformation response of joint shear panels in beam-column moment connections to concrete-filled tubes", *J. Struct. Eng.*, **130**(2), 244-252.
- Packer, J.A., Wardenier, J., Zhao, X.L., van der Vegte, G.J. and Kurobane, Y. (2009), *CIDECT Design Guide No. 3: Design Guide for Rectangular Hollow Section (RHS) Joints under Predominantly Static Loading*, (2nd edition), Bouwen met Staal, Switzerland.
- Park, S.H., Choi, S.M., Kim, Y.S., Park, Y.W. and Kim, J.H. (2010), "Hysteresis behavior of concrete filled square steel tube column-to-beam partially restrained composite connections", *J. Constr. Steel Res.*, **66**(7), 943-953.
- Prabhavathy, R.A. and Knight, G.M.S. (2006), "Behaviour of cold-formed steel concrete infilled RHS connections and frames", *Steel Compos. Struct., Int. J.*, **6**(1), 71-85.
- Qin, Y. and Chen, Z. (2016), "Research on cold-formed steel connections: A state-of-the-art review", *Steel Compos. Struct., Int. J.*, **20**(1), 21-41.
- Qin, Y., Chen, Z., Yang, Q. and Shang, K. (2014a), "Experimental seismic behavior of through-diaphragm connections to concrete-filled rectangular steel tubular columns", *J. Constr. Steel Res.*, **93**, 32-43.
- Qin, Y., Chen, Z. and Wang, X. (2014b), "Experimental investigation of new internal-diaphragm connections to CFT columns under cyclic loading", *J. Constr. Steel Res.*, **98**, 35-44.

- Qin, Y., Chen, Z. and Wang, X. (2014c), “Elastoplastic behavior of through-diaphragm connections to concrete-filled rectangular steel tubular columns”, *J. Constr. Steel Res.*, **93**, 88-96.
- Qin, Y., Chen, Z. and Rong, B. (2014d), “Component-based mechanical models for axially-loaded through-diaphragm connections to concrete-filled RHS columns”, *J. Constr. Steel Res.*, **102**, 150-163.
DOI: <http://dx.doi.org/10.1016/j.jcsr.2014.06.016>
- Qin, Y., Chen, Z., Wang, X. and Zhou, T. (2014e), “Seismic behavior of through-diaphragm connections between CFRT columns and steel beams-experimental study”, *Adv. Steel Constr.*, **10**(3), 351-371.
- Qin, Y., Chen, Z. and Han, N. (2014f), “Research on design of through-diaphragm connections between CFRT columns and HSS beams”, *Int. J. Steel Struct.*, **14**(3), 1-12.
- Ricles, J.M., Peng, S.W. and Lu, L.W. (2004), “Seismic behavior of composite concrete filled steel tube column-wide flange beam moment connections”, *J. Struct. Eng.*, **130**(2), 223-232.
- Rong, B., Chen, Z.H., Zhang, R.Y., Apostolos, F. and Yang, N. (2012), “Experimental and analytical investigation of the behavior of diaphragm-through joints of concrete-filled tubular columns”, *J. Mech. Mater. Struct.*, **7**(10), 909-929.
- Shams, M. and Saadeghvaziri, MA. (1997), “State of the art of concrete-filled steel tubular columns”, *ACI Struct. J.*, **94**(5), 558-571.
- Shanmugam, N.E. and Lakshmi, B. (2001), “State of the art report on steel-concrete composite columns”, *J. Constr. Steel Res.*, **57**(10), 1041-1080.
- Shin, K.J., Kim, Y.J., Oh, Y.S. and Moon, T.S. (2004), “Behavior of welded CFT column to H-beam connections with external stiffeners”, *Eng. Struct.*, **26**(13), 1877-1887.
- Shin, K.J., Kim, Y.J. and Oh, Y.S. (2008), “Seismic behaviour of composite concrete-filled tube column-to-beam moment connections”, *J. Constr. Steel Res.*, **64**(1), 118-127.
- Tang, J.R. (1989), *Seismic Resistance of Joints in Reinforced Concrete Frames*, Southeast University Press, Nanjing, China.
- Tizani, W., Al-Mughairi, A., Owen, J.S. and Pitrakkos, T. (2013a), “Rotational stiffness of a blind-bolted connection to concrete-filled tubes using modified Hollo-bolt”, *J. Constr. Steel Res.*, **80**, 317-331.
- Tizani, W., Wang, Z.Y. and Hajirasouliha, I. (2013b), “Hysteretic performance of a new blind bolted connection to concrete filled columns under cyclic loading: An experimental investigation”, *Eng. Struct.*, **46**, 535-546.
- Viest, I.M., Colaco, J.P., Furlong, R.W., Griffis, L.G., Leon, R.T. and Wyllie, L.A. (1997), *Composite Construction Design For Buildings*, McGraw-Hill Companies, Inc. and the American Society of Civil Engineers, USA.
- Wang, W.D., Han, L.H. and Zhao, X.L. (2009a), “Analytical behavior of frames with steel beams to concrete-filled steel tubular column”, *J. Constr. Steel Res.*, **65**(3), 497-508.
- Wang, J.F., Han, L.H. and Uy, B. (2009b-a), “Behaviour of flush end plate joints to concrete-filled steel tubular columns”, *J. Constr. Steel Res.*, **65**(4), 925-939.
- Wang, J.F., Han, L.H. and Uy, B. (2009b-b), “Hysteretic behaviour of flush end plate joints to concrete-filled steel tubular columns”, *J. Constr. Steel Res.*, **65**(8-9), 1644-1663.
- Wu, L.Y., Chung, L.L., Tsai, S.F., Shen, T.J. and Huang, G.L. (2005), “Seismic behavior of bolted beam-to-column connections for concrete filled steel tube”, *J. Constr. Steel Res.*, **61**(10), 1387-1410.
- Wu, L.Y., Chung, L.L., Tsai, S.F., Lu, C.F. and Huang, G.L. (2007), “Seismic behavior of bidirectional bolted connections for CFT columns and H-beams”, *Eng. Struct.*, **29**(3), 395-407.
- Zhao, X.L., Herion, S., Packer, J.A., Puthli, R.S., Sedlacek, G., Wardenier, J., Weynand, K., van Wingerde, A.M. and Yeomans, N.F. (2001), CIDECT Design Guide No. 8: Design Guide for Circular and Rectangular Hollow Section Welded Joints under Fatigue Loading, CIDECT and Verlag TÜV Rheinland GmbH, Köln, Germany.
- Zhou, T.H., He, B.K., Chen, G.J., Wei, C.W. and Shan, Y.M. (2004), “Experimental studies on seismic behavior of concrete-filled steel tubular column and steel beam joints under cyclic loading”, *J. Building Struct.*, **25**(1), 9-16.